Available online at www.sciencedirect.com
SCIENCE DIRECT®
Journal of Power Sources 129 (2004) 246–254
JOURNAL OF POWER SOURCES
www.elsevier.com/locate/jpowsour

Kinetics, simulation and insights for CO selective oxidation in fuel cell applications

Yongtaek Choi, Harvey G. Stenger*
Department of Chemical Engineering, Lehigh University, Bethlehem, PA 18015, USA

Received 20 October 2003; accepted 20 November 2003

Abstract

The kinetics of CO preferential oxidation (PROX) was studied to evaluate various rate expressions and to simulate the performance the CO oxidation step of a methanol fuel processor for fuel cell applications. The reaction was carried out in a micro reactor testing unit using a commercial Engelhard Selectoxo (Pt–Fe/γ-alumina) catalyst and three self-prepared catalysts. Temperature was varied between 100 and 300 °C, and a of range feed rates and compositions were tested. A reaction model in which three reactions (CO oxidation, H_2 oxidation and the water gas shift reaction) occur simultaneously was chosen to predict the reactor performance. Using non-linear least squares, empirical power-law type rate expressions were found to fit the experimental data. It was critical to include all three reactions to determine good fitting results. In particular, the reverse water gas shift reaction had an important role when fitting the experimental data precisely and explained the selectivity decrease at higher reaction temperatures. Using this three reaction model, several simulation studies for a commercial PROX reactor were performed. In these simulations, the effect of O_2/CO ratio, the effect of water addition, and various non-isothermal modes of operation were evaluated. The results of the simulation were compared with corresponding experimental data and shows good agreement.

Keywords: CO selective oxidation; PROX; Fuel processor; Fuel cell; Hydrogen; Water gas shift reaction

1. Introduction

Removing carbon monoxide in a hydrogen rich stream is a critical issue and an unavoidable problem when hydrocarbons are used as the hydrogen source for fuel cells. Regardless of the reformer, small amounts of CO exist after hydrocarbon reforming and even after the water gas shift reaction. These small amounts of CO, typically less than 1 mol%, must be removed to prevent poisoning of the fuel cell electrodes. Among the various methods to remove CO selectively, catalytic oxidation is considered as one of the most plausible and economical options. Due to the recent growth in research on fuel cells and fuel processing, a large number of studies on CO selective or preferential oxidation (PROX) have been published.

The catalysts for CO selective oxidation can be classified into three categories as shown in Fig. 1, which summarizes 30 recent publications [1–30]. The most commonly used formulation is platinum or other precious metals on alumina, and at temperatures around 200 °C. Also, Au based catalysts show good performance at lower temperatures around 100 °C which is close to PEM fuel cell operating temperatures. Lastly, several common transition metals have been investigated to find a more economical CO selective oxidation catalyst. Most recent papers are focus on catalyst formulation, characterization, and basic performance such as activity and selectivity of CO. Few papers have investigated the kinetics and rate expressions of the reactions involved.

In the CO selective oxidation reaction system, the following two oxidation reactions (1) and (2) occur.

$$\mathrm{CO} + \tfrac{1}{2}\,\mathrm{O_2} \rightarrow \mathrm{CO_2}, \qquad \Delta H^{\circ}_{298} = -283\,\mathrm{kJ/mol} \tag{1}$$

$$\mathrm{H_2} + \tfrac{1}{2}\,\mathrm{O_2} \rightarrow \mathrm{H_2O}, \qquad \Delta H^{\circ}_{298} = -242\,\mathrm{kJ/mol} \tag{2}$$

For precious metal catalysts, several different kinetic rate expressions have been reported. Amphlett et al. [4] developed a simple first-order rate expression for CO oxidation on a platinum/alumina catalyst as follows:

$$r_{\mathrm{CO}} = k_{\mathrm{CO}} C_{\mathrm{CO}} (\mathrm{mol\,s^{-1}\,kg^{-1}}),$$
$$\text{where } k_{\mathrm{CO}} = 0.026 \exp\left(-\frac{1000}{T}\right) (\mathrm{m^3\,s^{-1}\,kg^{-1}}) \tag{3}$$

* Corresponding author. Tel.: +1-610-758-4791; fax: +1-610-758-5057.
E-mail address: hgs0@lehigh.edu (H.G. Stenger).

0378-7753/$ – see front matter © 2003 Published by Elsevier B.V.
doi:10.1016/j.jpowsour.2003.11.038

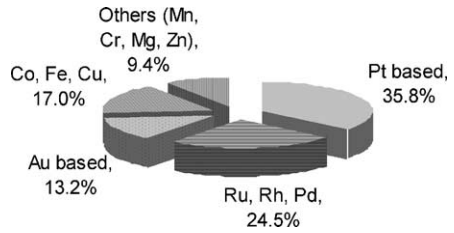

Fig. 1. Typical formulation of CO selective oxidation catalysts in the 30 recently published papers.

Kahlich et al. [7] derived a different kinetic expression by introducing a process parameter λ which is defined as the concentration ratio of oxygen to CO (Eq. (4)). According to this kinetic expression, the reaction rate of CO can be determined with reaction orders of −0.42 for CO and +0.82 for O_2 and an activation energy of 71 kJ mol^{-1}.

$$r_{CO} = k_1 P_{CO}^{0.42} \lambda^{0.82}, \qquad \text{where } \lambda = \frac{2C_{O_2}}{C_{CO}} = \frac{2P_{O_2}}{P_{CO}} \tag{4}$$

Also, Kim and Lim [20] used a similar rate expression as follows:

$$-r_{CO,TOF} = 1.4 \times 10^8 \exp\left(\frac{-78}{RT}\right) P_{CO}^{-0.51} P_{O_2}^{0.76} \tag{5}$$

In Table 1, the kinetic parameters of several empirical power law rate expressions are compared.

For another approach, Venderbosch et al. [9] (Eq. (6)) found the parameters of the Langmuir–Hinshelwood (LH) expression using a downhill-simplex minimization method and experimental data.

$$r(c,T) = \frac{k_p^0 \exp(-E_a/RT) c_{CO} c_{O_2}}{(1 + K_a^0 \exp(\Delta H_{ads}/RT) c_{CO})^2} \tag{6}$$

Finally, Sedmak et al. [27] evaluated two LH type rate expressions for the Cu-CeO based catalyst shown in Eqs. (7) and (8).

$$r_{CO} = \frac{k_{CO} k_{O_2} P_{CO} P_{O_2}^n}{0.5 k_{CO} P_{CO} + k_{O_2} P_{O_2}^n} \tag{7}$$

$$r_{CO} = \frac{k_L K_L P_{CO} P_{O_2}^m}{1 + K_L P_{CO}^n} \tag{8}$$

In spite of the many papers that give suggested rate expressions as described above, there are very few papers that consider H_2 oxidation simultaneously with CO oxidation reaction in PROX related publications.

Rate expressions for hydrogen-oxidation reaction over the platinum catalyst have been found separately in several publications [31–33]. The rate expressions of power law type empirical expressions are summarized in the Table 1b. As shown in these rate expressions, the H_2 oxidation reaction rate mainly depends on the partial pressure of oxygen and not the partial pressure of hydrogen.

The feed stream of a PROX reactor in a methanol fuel reformer system is composed of H_2, O_2, CO, CO_2 and H_2O. Therefore in addition to the reactions of CO and H_2 oxidation, it is also necessary to consider the reverse water gas shift reaction in the kinetic model of the PROX reactor.

$$H_2O + CO \leftrightarrow CO_2 + H_2, \qquad \Delta H_{298}^{\circ} = -41.1\,\text{kJ/mol} \tag{9}$$

The equilibrium constant of the water gas shift reaction is about 225 at 200 °C suggesting the forward reaction should be dominant in this temperature region if the gas does not have large amounts of $H_2$and CO_2. However, in most PROX reactor feed gases, the concentration of H_2 and CO_2 are approximately 70 and 20%, respectively, which are high enough to influence the reverse WGS reaction. Therefore, to accurately predict the concentration of all gas components, all three reactions (CO oxidation, H_2 oxidation and (reverse) water gas shift reaction) must be considered simultaneously.

This three reaction system and the exact rate expressions for each reaction are important components in the optimization and control of commercial fuel reformers. The goals of this study are to determine the kinetic models, to find the exact rate parameters, and to simulate the CO selective oxidation system. Through this approach, we hope to gain

Table 1
Empirical expressions for CO and H_2 oxidation in the literature

Catalyst	α	β	ln(k_0)	E (kJ mol^{-1})	Reference
(a) For CO oxidation rate: $r = k_0 \exp(-E/RT) P_{O_2}^{\alpha} P_{CO}^{\beta}$					
Pt/γ-Al_2O_3	0.8	−0.4		72–76	[7]
	1	−1.5	–	55	Muraki [7]
	0.7	−0.1		67–71	Sarkany [7]
Pt/SiO_2	1	−1 to 0		56–80	
Au/α-Fe_2O_3	1	1		31	[11]
$Cu_{0.1}Ce_{0.9}O_{2-y}$			11.88	57.2	[27]
	γ	δ			
(b) For H2 oxidation rate: $r = k_0 \exp(-E/RT) P_{H_2}^{\gamma} P_{O_2}^{\delta}$					
Pt/γ-Al2O3	0	0.8		21.9	[31]
Pt/γ-Al2O3	0	1	–	20.9–58.8	[32]
Pt(1,1,1)	–	0.59	–	14.3–47.0	[33]

important beneficial insights for the design and operation of the PROX reactor in a fuel cell system.

2. Experimental

2.1. Catalysts and reactors

For the experiments in this study, a commercial catalyst and several in house prepared catalysts have been tested. Reaction conditions are chosen similar to the reactor conditions which would be found in a fuel processor system, such as: feed gas flow rate and composition, space velocity, pressure, and reactor temperature. The commercial catalyst used was the Selectoxo catalyst manufactured by Engelhard ($Pt–Fe/Al_2O_3$). The Selectoxo catalyst is a 3 mm × 4 mm sized pellet catalyst composed of 0.5% Pt and 0.02% Fe on a γ-alumina support. The catalysts pellets were ground lightly to a particle diameter of 100–250 μm to eliminate internal diffusion resistance but allow good gas distribution.

Three different in-house catalysts, Pt, Rh, and Pt–Rh over the γ-alumina were prepared. The platinum catalyst was made from an aqueous solution of hydrogen hexachloro-platinate(IV) hydrate (Aldrich Chemical Co.), and the rhodium catalyst was made from rhodium(III) chloride hydrate (Aldrich Chemical Co.) both by the conventional impregnation method. The amounts of metal loading after the impregnation were respectively 0.55% Pt, 0.74% Rh, and 0.55% Pt–0.07% Rh. After the impregnation, all three catalysts were dried at 120 °C for 12 h and calcined at 450 °C for 3 h. Because the CO and H_2 oxidation reactions are highly exothermic, 0.5 g of each catalyst was diluted with 5.0 g of inert alumina to maintain isothermal conditions.

All reaction tests were performed in a standard catalyst test unit. A stainless steel (or glass) tubular reactor, 1/2 in. in diameter and 12 in. long was used for all reaction tests. To ensure isothermal conditions along the bed length, a split tubular furnace was used and the temperature of the catalyst bed was measured directly by a 1/16 in. J-type thermocouple.

2.2. Conditions and product analysis

To simulate the conditions exiting the water gas shift reactor in a methanol reforming unit, the feed gas stream contained 62–72% H_2, 0.5–5.0% O_2, 2–17% N_2, 0.5–3.0% CO, and 20–24% CO_2 (dry basis). In cases when water is added, the injection rates were controlled precisely by a syringe pump, 74900 Series (Cole Palmer), from 0.5 to 8 ml h^{-1}. The reaction tests were performed at temperatures between 100 and 300 °C. With these catalyst loadings and feed compositions, the GHSV at reaction temperature was controlled between 1000 and 20,000 h^{-1}. All the reaction runs were performed under atmospheric pressure.

The effluent of the reactor was connected directly to a CARLE Series S gas chromatograph containing a thermal conductivity detector using helium as the carrier gas. The column, a Supelco Carboxen 1000 (60–80 mesh, 15 ft × 1/8 in.), was used to analyze the light gas components. The GC chamber was maintained at a constant temperature of 50 °C to separate N_2 and O_2 properly. Five components H_2, O_2, N_2, CO and CO_2 were measured during each test run. Material balances on carbon were calculated to verify measurement accuracy, and for all runs reported here were within 3% of closure.

Table 2
Feed composition and catalysts in the experiment

Run No.	Feed mixture (mol%)		Catalysts	Water
	CO	O_2		
1–3	∼3%	3%, 5%, 1.5%	Pt–Fe (Selectoxo)	–
4	∼1%	1%	Pt–Fe	–
5–6	∼0.6%	1.2%, 0.6%	Pt–Fe	–
7–9	∼1%	1%	Pt 0.55, Rh, Pt–Rh	–
10–11	∼1%	1%	Pt 0.19%, Pt 1.6%	–
12–13	∼1%	1%	Pt–Fe	15%, 7%

2.3. Activity and selectivity measurements

CO activity and selectivity (moles of CO oxidized divided by two times the moles of O_2 consumed) were measured at various levels of CO, O_2, and water. The catalysts and feed streams of 14 runs are summarized in Table 2. The oxygen level (air addition rate) is an important factor in PROX operation. Theoretically only 0.5 mol of oxygen is needed to remove one mole of CO. However, most of PROX reactors use excess air to some extent due to H_2 oxidation reaction. Because CO concentrations entering a commercial PROX reactor are usually less than 1%, we varied the CO concentration from 0.5 to 3.0% and varied the O_2 concentration from 0.5 to 6.0%.

In each run, five to eight different temperatures (under 300 °C) were selected. At temperatures under 150 °C, it was difficult to get repeatable data because of low conversion and temperature fluctuations between the catalyst surface and the reactor. Therefore, most of the data in this low temperature range were obtained by averaging 12–24 h of data at the targeted temperature. CO conversion was calculated directly from the concentration change of CO. The selectivity of CO in the PROX reactor was defined as follows.

$$\text{Selectivity (\%)} = \frac{0.5(n_{CO}^{in} - n_{CO}^{out})}{n_{O_2}^{in} - n_{O_2}^{out}} \times 100$$

3. Experimental results

3.1. CO activity and selectivity over a commercial catalyst

Fig. 2(a) and (b) show a plots of CO conversion and selectivity at various O_2/CO feed ratios as a function of re-

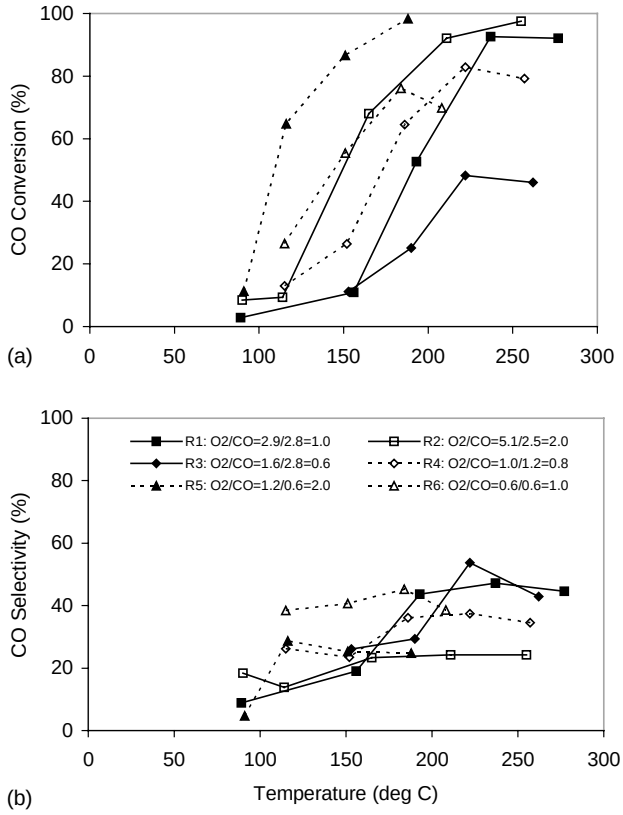

Fig. 2. Activity and selectivity for CO selective oxidation with various O_2/CO ratio as a function of reaction temperature: 0.5 g of Selectoxo (Pt–Fe/γ-alumina) catalyst, flow rate = 167 sccm, H_2 = 64–75 mol%, O_2/CO in mol%, 1 atm, no water addition.

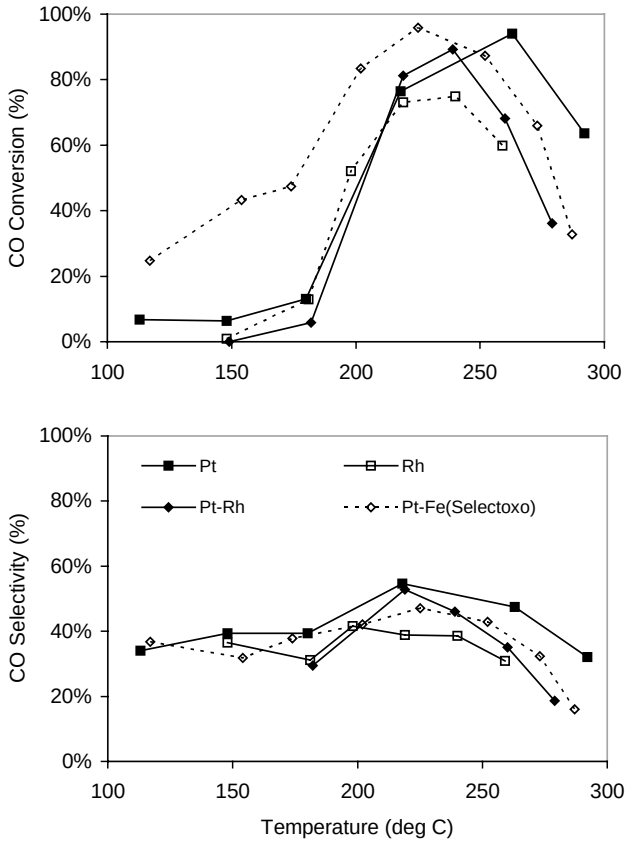

Fig. 3. Activity and selectivity for CO selective oxidation with various catalyst formulations as a function of reaction temperature: 0.5 g of catalysts (0.55% Pt, 0.78% Rh, 0.55% Pt–0.07% Rh, and 0.5% Pt–0.02% Fe), flow rate = 167 sccm, H_2 = 72.0 mol%, O_2 = 1.0 mol%, CO = 1.0 mol%, CO_2 = 22 mol%, 1 atm, no water addition.

action temperature for the Selectoxo catalyst. As shown in this figure, the conversion of CO increases at high O_2/CO ratios and low CO concentrations. When the O_2/CO ratio was 2.0, the maximum CO conversion was more than 95% even under 200 °C (see R2, R5). In the three cases, where the O_2/CO mole ratio is near 1.0, lower CO concentrations gave higher CO conversions (see R4, R6). However, selectivity was low when the O_2/CO ratio was high (see R2, R5). When the O_2/CO ratio is around one or less, the selectivity of the catalyst has a maximum value between 200 and 250 °C (see R1, R3).

3.2. Other precious metal PROX catalysts

The performance of three in-house catalysts is compared with the commercial Pt–Fe catalyst in Fig. 3. Rhodium is a common catalyst used for oxidation reactions and one of the candidates for the CO PROX reaction. Although Rh is used for automotive catalysts, there are very few papers addressing CO selective oxidation for Pt–Rh bimetallic catalysts. Cai et al. [34] reported the synergist effects of Pt–Rh alloy particle at certain conditions for CO oxidation. However, that work was when hydrogen was not a feed component. As shown in Fig. 3, the rhodium catalyst has a lower activity than any of the Pt catalysts. The bimetallic catalyst (Pt 0.55 wt.%–Rh 0.07 wt.%) shows no synergetic effect and gives almost the same results as the Pt (0.55 wt.%) catalyst. The Pt–Fe catalyst has the highest CO conversion and the rhodium catalyst shows the lowest selectivity values. The only surprising result in Fig. 3 is that the platinum catalyst shows a slightly better selectivity at temperatures above 250 °C.

Fig. 4 shows the activity of the in house platinum catalyst with varying Pt loading (1.6, 0.55 and 0.19% Pt). As expected, the activity directly increases with platinum amount over this range of Pt loadings. However, the high loading platinum catalyst (1.6%) shows the poorest selectivity at higher temperatures.

3.3. Water addition effect

Water content is one of the most critical factors in the PROX reaction and is very important for proper operation of the fuel cell stack. Contradictory viewpoints still exist as to whether water acts positively for CO oxidation or not. Many research groups [8,21,22] have reported that water enhances the CO oxidation reaction for a certain range of temperatures. On the other hand, Korotkikh and Farrauto reported

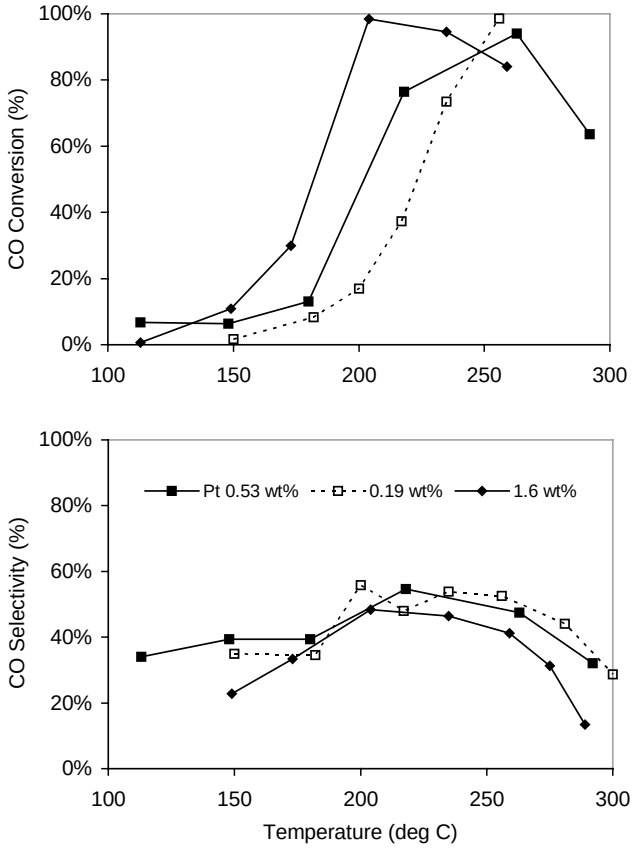

Fig. 4. Activity and selectivity for CO selective oxidation with various platinum loadings as a function of reaction temperature: 0.5 g of catalysts, platinum loading in weight %, flow rate = 167 sccm, H_2 = 72.0 mol%, O_2 = 1.0 mol%, CO = 1.0 mol%, CO_2 = 22 mol%, 1 atm, no water addition.

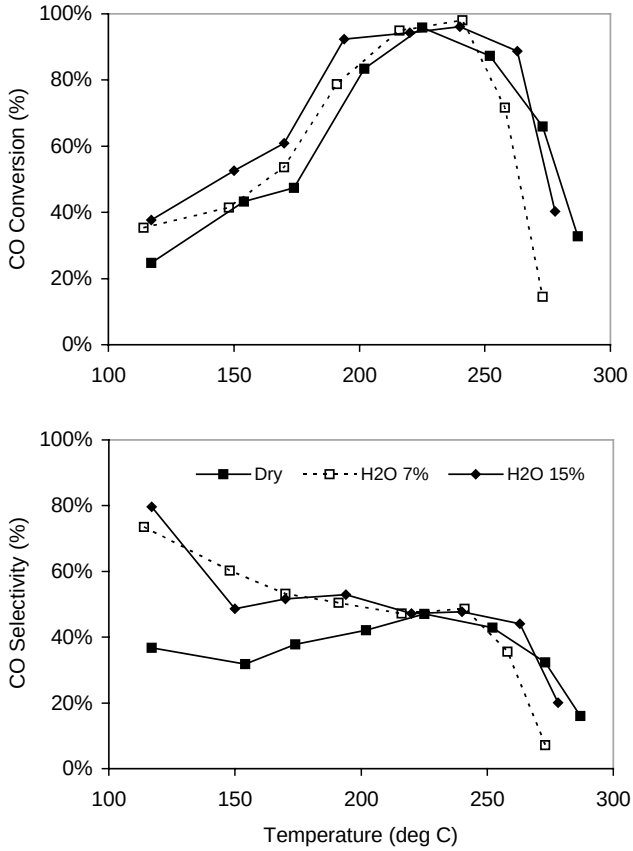

Fig. 5. Activity and selectivity for CO selective oxidation with addition of water as a function of reaction temperature: 0.5 g of Selectoxo (Pt–Fe/γ-alumina) catalyst, flow rate = 167 sccm, H_2 = 72.0 mol%, O_2 = 1.0 mol%, CO = 1.0 mol%, CO_2 = 22 mol%, 1 atm.

that the addition of small amounts of water (3 mol%) decreased the CO conversion. Grisel and Nieuwenhuys [19] and Avgouropoulos et al. [24] also reported that H_2O had a detrimental effect on the CO oxidation activity of Au based catalyst.

In this study, as shown in Fig. 5, the activity and selectivity increases with water addition up to the temperature of 220 °C for water addition of 15% or 7% (mol%). Above 220 °C, large amounts of water had a positive effect on selectivity and activity while smaller amounts of water were detrimental compared to the dry case. The reasons for these water effects are discussed in the following section.

4. Kinetics and simulations

4.1. Kinetics and rate expressions for the PROX reactions

As described previously, this study is distinctive in that it addresses all three reactions in the CO oxidation system: H_2 oxidation, water gas shift reaction, and CO oxidation. For the water gas shift reaction (3), the kinetics is well known and it is reliable to write a rate expression as follows [35]:

$$-r_3 = k_3\left(P_{CO}P_{H_2O} - \frac{P_{CO_2}P_{H_2}}{K_P}\right),$$
$$\text{where } K_P = \exp\left(\frac{4577.8}{T} - 4.33\right) \quad (10)$$

The H_2 oxidation reaction (2) in a hydrogen rich environment can be modeled using an empirical rate expression similar to others [31–33].

$$-r_2 = k_2 P_{O_2}^{\gamma} \quad (11)$$

And an empirical expression can be adequately used for the rate of CO oxidation (1).

$$-r_1 = k_1 P_{CO}^{\alpha} P_{O_2}^{\beta} \quad (12)$$

The constants in each rate expression are assumed to be Arrhenius functions of temperature ($A_o \exp(-E/RT)$), which gives nine parameters (three frequency factors, three activation energies, and two power constants) to be found for the complete model. All forty data sets shown in previous graphs were used to find these nine parameters.

By using data at constant temperature, the values of α, β, γ, k_1, k_2, and k_3 were determined by minimizing the sum of

the square of the difference between predicted and observed CO conversion (Eq. (7)).

$$\text{Minimize}\left\{\sum_{i=1}^{N}(\text{Xe}_{\text{CO},i}-\text{Xc}_{\text{CO},i})^2\right\} \tag{13}$$

where i = experiment number ($N = 28$ for CO selective oxidation), $\text{Xe}_{\text{CO},i}$ = experimental CO conversion at the reactor outlet (mol/h), and $\text{Xe}_{\text{CO},i}$ = calculated CO conversion at the reactor outlet (mol/h).

This procedure found that the best power law exponents were 0.5 for O_2 and −0.1 for CO. Fixing the exponents at these values, all of data (40 sets) were fit simultaneously by varying the activation energies and pre-exponential factors to again minimize the sum of squares error (Eq. (7)). To obtain the exiting concentrations for each experiment, the MATLAB subroutine function ODE23 was used for numerical integration. To minimize Eq. (7), the MATLAB subroutine function LSQNONLIN was used for non-linear least squares optimization.

The empirical rate expressions derived from this numerical analysis are as follows:

$$-r_1 = 3.528\times10^2\exp\left(\frac{-33092}{RT}\right)P_{\text{O}_2}^{0.5}P_{\text{CO}}^{-0.1} \tag{14}$$

$$-r_2 = 2.053\times10\exp\left(\frac{-18742}{RT}\right)P_{\text{O}_2}^{0.5} \tag{15}$$

$$-r_3 = 4.402\times10^3\exp\left(\frac{-34104}{RT}\right)\times\left(P_{\text{CO}}P_{\text{H}_2\text{O}}-\frac{P_{\text{CO}_2}P_{\text{H}_2}}{K_{\text{P}}}\right) \tag{16}$$

The quality of the fit is shown in Fig. 6 by comparing the observed and calculated CO conversion and selectivity for all the experiments. As shown in the figure, the calculated values show good agreement with the experimental values. The R^2 values for CO conversion was 0.92 for all data sets. Although selectivity was not specifically fit, the calculated values from the simulation are located within ±10% errors range for most experimental data.

As shown in Table 1, literature values of the power constants for CO oxidation are 0.7–1.0 for oxygen, and −1.5 to 0 for CO, and the activation energy for CO oxidation is between 55 and 80 kJ mol^{-1}. The rate parameters from this study have a slightly lower value for O_2 order and activation energy. To address this concern, the experimental data was fit using only one reaction (CO oxidation). In that approach, the resulting best-fit power constant for oxygen was 0.76, which is similar to the values in the literature, and a higher activation energy of 46 kJ mol^{-1} was found. However, without using all three reactions, the simulated values for CO conversion did not compare well with the experimental data and showed a severe disagreement with the selectivity data. After including the reverse water gas shift reaction and using the three reaction model, the calculated values from the simulation were almost exactly matched with the experimental data.

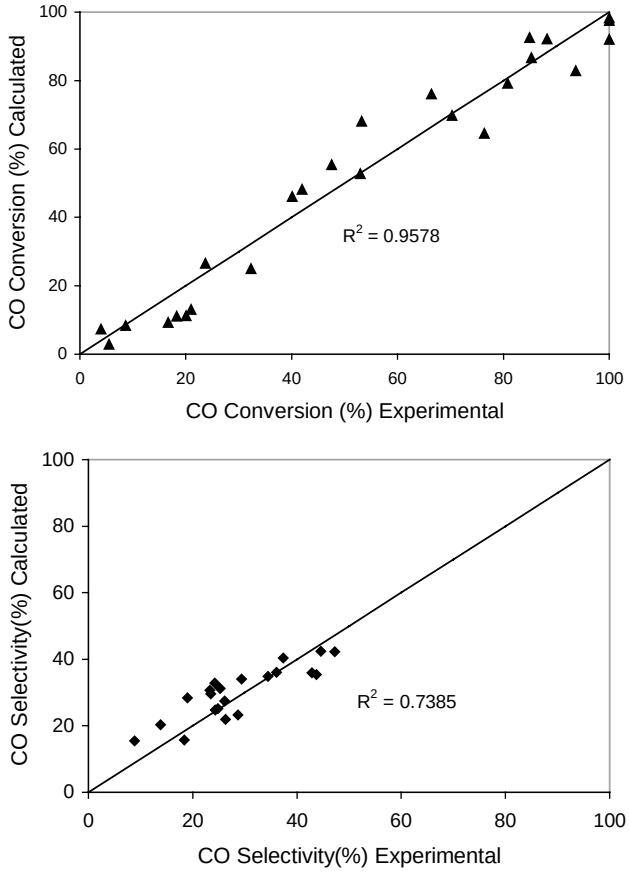

Fig. 6. Comparison of experimental exiting CO conversion and selectivity data with calculated numerical value from three rate expressions obtained this study. 0.5 g of Selectoxo (Pt–Fe/γ-alumina) catalyst, flow rate = 167 sccm, H_2 = 62–72 mol%, O_2/CO = 0.5–2.0, reaction temperature = 100–300 °C, 1 atm, no water addition.

A hypothetical cause of decreasing selectivity at higher temperatures might be that the activation energy for H_2 oxidation is greater than the activation energy for CO oxidation. However, it was impossible to fit the data accurately if we constrained the activation energy in this manner. Rather, we found the activation energy of the H_2 oxidation reaction to be lower (one-half) than that for CO oxidation. This further validates our need to include the WGS reaction since this is the only other reason why selectivity would decrease at increasing temperatures.

4.2. PROX reactor simulations and heat balance insights

Using the rate expressions obtained above, a series of simulations of the PROX reactor were run based on a 1 kW fuel cell/fuel reformer system. Design parameters and operating conditions of the 1 kW system are summarized in the Table 3. For this system, 11.1 mol h^{-1} of methanol must be fed to the methanol reformer. If CO is reduced to the

Table 3
Design basis for PROX reactor and 1 kW fuel cell system

	Design variables	Values	Unit
PROX reactor	CO inlet molar flow rate	0.443	gmol h^{-1}
WGS reactor	CO inlet molar flow rate	11.1	gmol h^{-1}
	H2 inlet molar flow rate	22.2	gmol h^{-1}
	CO target conditions	1	mol%
Fuel reformer	Required amount of hydrogen	33.3	gmol h^{-1}
	Methanol feed rate	11.1	gmol h^{-1}
Fuel cell stack	Target power	1	kW
	Stack voltage (50 cells)	35	V
	Cell amperage	28.57	A
	Fuel cell efficiency, assumed	80	%

level of 1 mol% through the WGS reactor, then the expected inlet concentration of CO to the PROX reactor would be 0.443 gmol h^{-1}.

The performance of the PROX reactor for this basis is shown in Fig. 7. This Figure plots reactor temperature, CO concentration, CO conversion, and CO selectivity along the reactor path (catalyst weight) for a feed temperature of 200 °C. Because both CO oxidation and H_2 oxidation are exothermic, the reactor temperature must be actively controlled. Four different heat exchange cases are considered: (1) perfect isothermal operation, (2) adiabatic operation and (3, 4) actively cooled with two heat transfer rate coefficients. For isothermal operation, the CO conversion gradually reached 95% at the reactor exit while the CO selectivity remained almost constant at approximately 40%. If adiabatic operation is assumed, the reactor temperature increases to a maximum 372 °C near the middle of the reactor, and then decreases slowly due to the endothermic effects of the reverse WGS reaction. For the adiabatic case, the CO activity and selectivity decrease rapidly after the maximum temperature, with a maximum CO conversion of approximately 76%. The decreasing conversion and selectivity are due to the reverse WGS reaction since the oxygen has been completely consumed.

Also shown in Fig. 7 are two cases with a simple heat exchange model represented by $Ua = 15$ and 30 J s^{-1} cm^{-3} K^{-1}. The overall heat transfer coefficient (U) is combined with characteristic diameter of the reactor ($a = 4/D$) and it is applied to the energy balance for a steady state non-isothermal tubular reactor.

$$\frac{dT}{dW} = \frac{Ua(Tw - T) + (-\Delta H_{Rx})(-r_i)}{\sum n_i C_{pi}} \quad (17)$$

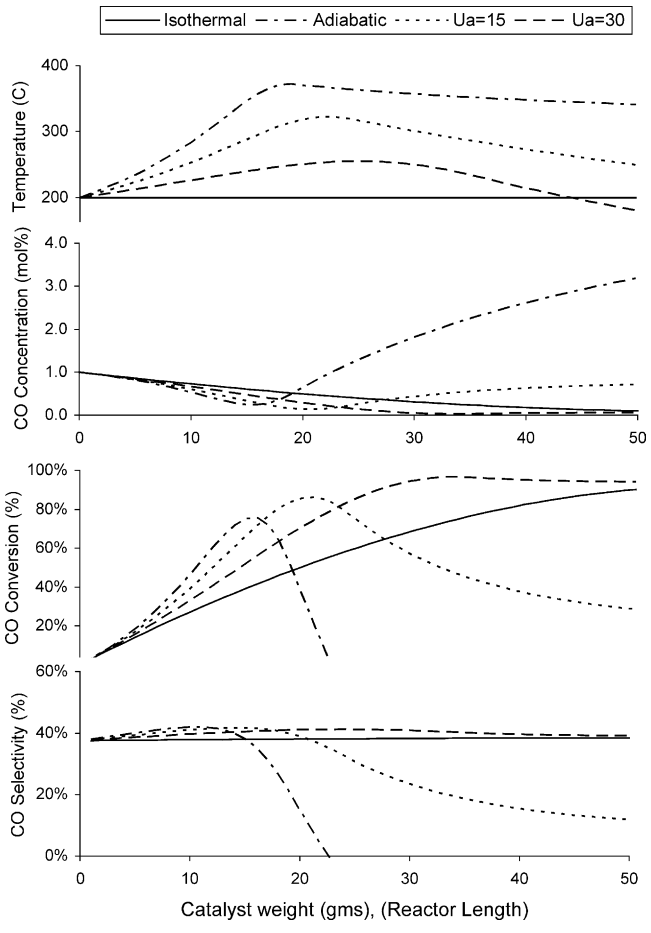

Fig. 7. PROX reactor simulation with various heat transfer cases using 50 g of Selectoxo catalyst, feed $H_2 = 33$ gmol h^{-1}, $O_2/CO = 1.2$, water addition = 10%, and inlet temperature = 200 °C, $Ua = 0$, 15, 30, ∞ (J s^{-1} cm^{-3} K^{-1}). Note that negative conversion and selectivity are not shown.

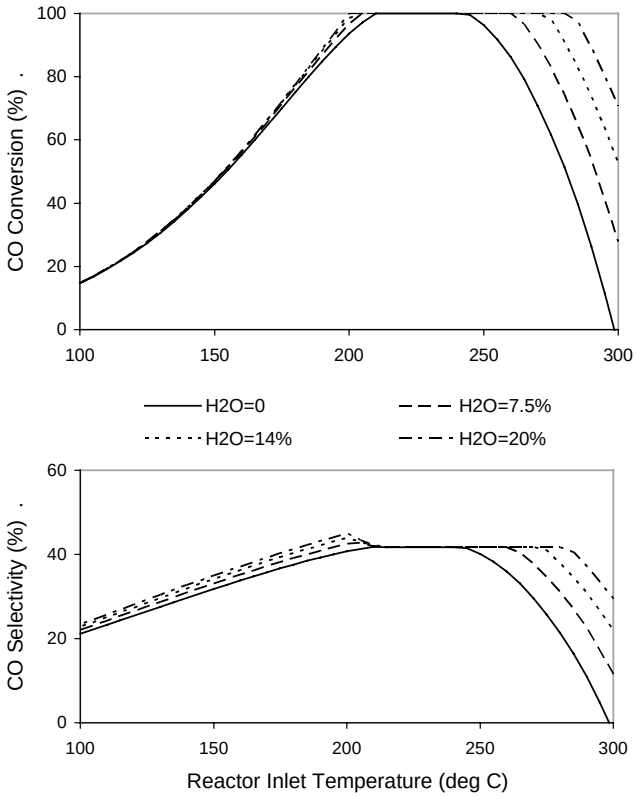

Fig. 8. Exiting concentration and selectivity with the addition of water versus reactor temperature using 50 g of Selectoxo catalyst, $H_2 = 33$ gmol h^{-1}, $O_2/CO = 1.2$, 1% CO.

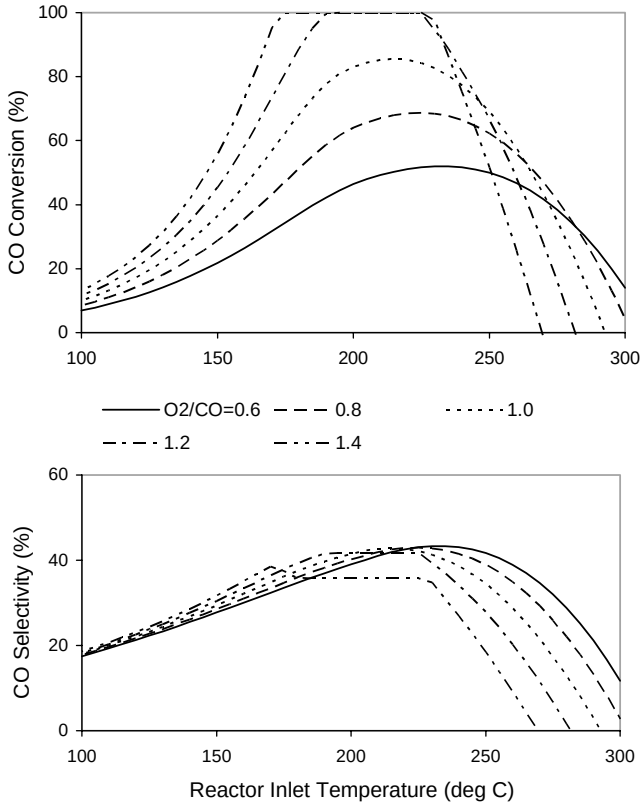

Fig. 9. CO Conversion and selectivity at various O_2/CO ratios versus reactor temperature: 50 g of Selectoxo catalyst, $H_2 = 33\,\mathrm{gmol\,h^{-1}}$, water = 10%, 1% CO.

For the case of $Ua = 30\,\mathrm{J\,s^{-1}\,cm^{-3}\,K^{-1}}$, the CO conversion and selectivity was higher than the isothermal, adiabatic or $Ua = 15\,\mathrm{J\,s^{-1}\,cm^{-3}\,K^{-1}}$ cases. These results show how important it is to properly design the heat transfer system to maximize the performance of the PROX reactor.

4.3. The effects of water addition and O_2/CO ratio

Fig. 8 shows the effects of water feed on CO conversion and selectivity for isothermal operation at a range of temperature. As shown in the figure, the CO conversion is enhanced by the addition of water when the reactor temperature is above 200 °C. Also the temperature window where 100% CO conversion is attainable becomes wider as more water is added and the selectivity remains unchanged at approximately 40% in this window. This positive influence of adding water is consistent with our experimental results and others. Manasilp and Gulari [22] suggested that the addition of water reduces the activation energy for CO oxidation. Also, they suggested three possibilities for water enhancement: (1) the water gas shift reaction, (2) the role of the adsorbed hydroxyl group, or (3) the change of Pt metal state. Our simulations show that the reverse WGS is most likely the cause of this enhancement.

Fig. 9 shows the effects of varying the O_2/CO feed ratio. To reach 100% CO conversion, the O_2/CO ratio must be greater than one. For CO selectivity higher O_2/CO ratio is advantageous at low temperatures while a lower ratio is better at higher temperatures, due to the competing effects of the two oxidation reactions.

In summary these results suggest the best operation will be achieved at an O_2/CO ratio of 1.0–1.2, an isothermal reactor temperature of 200–220 °C, and a feed water content above 20%.

5. Conclusion

A three reaction model consisting of CO oxidation, H_2 oxidation, and the water gas shift reaction is necessary to understand the behavior of the PROX reaction system. Empirical rate expressions for the reactions were accurately derived from a large set of experimental data, using a commercial Pt–Fe catalyst. Applying these empirical relationships in a simple tubular reactor model, it was possible to gain insights into the design and operation of the PROX reactor. The trend of decreasing CO conversion and selectivity at higher temperatures is accurately predicted to be caused by the reverse water gas shift reaction rather than a difference in the activation energies for CO oxidation and H_2 oxidation. Also, it is shown that adding water should increase the performance of PROX reactors. The results of this study are expected to be a critical part of the overall design, optimization and control of a fuel cell and fuel reformer system.

Acknowledgements

The authors thank the APERG sponsorship from Air & Waste Management Association and Engelhard Corporation for the catalyst.

References

[1] M.L. Brown, Ind. Eng. Chem. Res. 52 (1960) 841–844.
[2] S.H. Oh, R.M. Sinkevitch, J. Catal. 142 (1993) 254–262.
[3] K. Omata, T. Takada, S. Kasahara, M. Yamada, Appl. Catal. A: Gen. 146 (1996) 255–267.
[4] J.C. Amphlett, R.F. Mann, B.A. Peppley, Int. J. Hydrogen Energy 21 (8) (1996) 673–678.
[5] R. Sanchez, A. Ueda, K. Tanaka, M. Haruta, J. Catal. 168 (1997) 125–127.
[6] H. Igarashi, H. Uchida, M. Suzuki, Y. Sasaki, M. Watanabe, Appl. Catal. A: Gen. 159 (1997) 159–169.
[7] M.J. Kahlich, H.A. Gasteiger, R.J. Behm, J. Catal. 171 (1997) 93–105.
[8] R.H. Nibbelke, M.A.J. Campman, J.H.B.J. Hoebink, G.B. Marin, J. Catal. 171 (1997) 358–373.
[9] R.H. Venderbosch, W. Prins, W.P.M. Swaaij, Chem. Eng. Sci. 53 (19) (1998) 3355–3366.
[10] S. Kawatsu, J. Power Sources 71 (1998) 150–155.
[11] M.J. Kahlich, H.A. Gasteiger, R.J. Behm, J. Catal. 182 (1999) 430–440.

[12] M.M. Schubert, M.J. Kahlich, H.A. Gasteiger, R.J. Behm, J. Power Sources 84 (1999) 175–182.
[13] B. Rohland, V. Plzak, J. Power Sources 84 (1999) 183–186.
[14] Y. Teng, H. Sakurai, A. Ueda, T. Kobayashi, Int. J. Hydrogen Energy 24 (1999) 355–358.
[15] C.D. Dudfield, R. Chen, P.L. Adcock, J. Power Sources 85 (2000) 237–244.
[16] C.D. Dudfield, R. Chen, P.L. Adcock, J. Power Sources 86 (2000) 214–222.
[17] G.K. Bethke, H.H. Kung, Appl. Catal. A: Gen. 194 (2000) 43–53.
[18] O. Korotkikh, R. Farrauto, Catal. Today 62 (2000) 249–254.
[19] R.J.H. Grisel, B.E. Nieuwenhuys, J. Catal. 199 (2001) 48–59.
[20] D.H. Kim, M.S. Lim, Appl. Catal. A: Gen. 224 (2002) 27–38.
[21] Y. Hasegawa, A. Ueda, K. Kusakabe, S. Morooka, Appl. Catal. A: Gen. 225 (2002) 109–115.
[22] A. Manasilp, E. Gulari, Appl. Catal. B: Environ. 37 (2002) 17–25.
[23] J.B. Wang, S.C. Lin, T.J. Huang, Appl. Catal. A: Gen. 232 (2002) 107–120.
[24] G. Avgouropoulos, T. Ioannides, Ch. Papadopoulou, J. Batista, S. Hocevar, H.K. Matralis, Catal. Today 75 (2002) 157–167.
[25] W.S. Epling, P.K. Cheekatamarla, A.M. Lane, Chem. Eng. J. 4050 (2002) 1–8.
[26] X. Liu, O. Korotkikh, R. Farrauto, Appl. Catal. A: Gen. 226 (2002) 293–303.
[27] G. Sedmak, S. Hocevar, J. Levec, J. Catal. 213 (2003) 135–150.
[28] P.V. Snytnikov, V.A. Sobyanin, V.D. Belyaev, P.G. Tsyrulnikov, N.B. Shitova, D.A. Shlyapin, Appl. Catal. A: Gen. 239 (2003) 149–156.
[29] J. Zhang, Y. Wang, B. Chen, C. Li, D. Wu, X. Wang, Energy Conversion Manage. 44 (2003) 1805–1815.
[30] A. Worner, C. Friedrich, R. Tamme, Appl. Catal. A: Gen. 6464 (2003) 1–14.
[31] J.A. Maymo, J.M. Smith, AIChE J. 12 (5) (1996) 845–854.
[32] K.W. Hansen, S.B. Jorgensen, Chem. Eng. Sci. 31 (1976) 579–686.
[33] L.K. Verheij, Surf. Sci. 371 (1997) 100–110.
[34] Y. Cai, H. Stenger, C. Lyman, J. Catal. 161 (1996) 123–131.
[35] Y. Choi, H. Stenger, J. Power Source 124 (2) (2003) 432–439.